

# Seismic Upgrade of an Existing Tall Building by Different Energy Dissipation Devices

*Shanshan Wang, Graduate Student Researcher  
Stephen Mahin, Professor  
University of California, Berkeley  
Berkeley, CA*

## Abstract

The Pacific Earthquake Engineering Research (PEER) Center has expanded its Tall Building Initiative (TBI) program to include the seismic performance of existing tall buildings. A 35-story steel moment resisting frame, designed in 1968, and had representative details of buildings between 1960 to 1990 was selected for detailed seismic evaluation in the framework of Performance Based Earthquake Engineering (PBEE). It was identified that the case study building failed to meet the performance objectives suggested by ASCE 41-13, and had a number of seismic vulnerabilities that endangered its structural integrity at two basic safety earthquake hazard levels (BSE): BSE-1E and BSE-2E. Therefore, exploration of retrofit strategies and their cost-effectiveness are fostered. In this paper, three kinds of supplemental energy dissipation devices are investigated to upgrade the seismic performance of the case study building, including fluid viscous dampers (FVDs), viscous wall dampers (VWDs) and buckling restrained braces (BRBs). The retrofit design started by selecting locations to install supplemental devices. Then the total effective damping ratios needed to achieve the target roof displacements in two directions were estimated based on a damping scale factor (DSF). One retrofit strategy by using FVDs was investigated as a first trail, and the mechanical characteristics of each damper device were calculated based on the overall effective damping ratio and the story wise distributions of dampers. Next, other two retrofit strategies by using VWDs or BRBs were investigated. Sizing of different devices at one location was performed following the principle of equal energy dissipation. The effectiveness of each strategy to meet the retrofit intent of ensuring structural stability at BSE-2E were compared. Moreover, probabilistic damage and loss analysis were conducted using Performance Assessment Calculation Tool (PACT) to relate the structural responses to economic losses. After a detailed examination, it was found that upgrading the case study tall building using FVDs was the most effective retrofit strategy to control structural responses, and reduce damage and economic losses after BSE-2E events.

## 01. Introduction

In traditional design where seismic energy is mainly dissipated by irrecoverable inelastic deformation of structural elements, the building safety is maintained at the compromise of components' damage, leading to direct and indirect economic losses. This has been highlighted in recent earthquakes in Chile, Japan, China and New Zealand. As such, the development of seismic protection systems has been spurred, which includes base isolation, active control and passive energy dissipation systems by large (Soong and Spencer, 2002). Of these, passive energy dissipation systems do not require external power source, and are relatively easy to install, and thus considered as a better choice to upgrade existing structures. Three kinds of devices are investigated in this paper: fluid viscous dampers (FVDs), viscous wall dampers (VWDs) and buckling restrained braces (BRBs), and they are used in combination with preliminary retrofit methods to upgrade an existing 35-story Pre-Northridge steel moment resisting frame. The investigations focus on comparing the cost-effectiveness of each retrofit method, and also raise critical design considerations that appear for each strategy. Fig. 1 illustrates the applications of these three devices.



(a). FVDs

Figure 1. Supplemental energy dissipation devices



(b). VVDs



(c). BRBs

Figure 1 (continued). Supplemental energy dissipation devices

## 02. Evaluation of the Case Study Building

A 35-story steel moment resisting frame that had representative design details from the period of 1960 to 1990 was selected for systematic seismic evaluations. The case study building is about 490 ft. tall, with a typical floor height of 13 ft. It spans about 185 ft. by 135 ft. in plan, and has a typical beam span of 30 ft. The building completed construction in San Francisco in 1971, consisting of complete three-dimensional moment-resisting space frames in both longitudinal direction ( $X$ ) and transverse direction ( $Y$ ). Fig. 2 shows a frame elevation and a floor plan of the building model.

Beam-to-column moment connections used typical pre-Northridge details and the column slices were erected using partial joint penetration welds, both considered to be quite brittle. A three-dimensional (3D) model was generated using the program: Open System for Earthquake Engineering Simulation (OpenSees, McKenna et. al., 2010) to investigate its nonlinear dynamic behavior; see Fig. 3. All aboveground main framing members contributing to the seismic lateral force resisting systems were included (see Fig. 2 and Fig. 3). Given the nature of this investigation, certain modelling simplifications were made. For instance, the basement levels were disregarded. The first three elastic modal periods of the structure were: 4.70 sec. ( $X$ -direction translation), 4.53 sec. ( $Y$ -direction translation), and 4.15 sec. (rotation). More details about the building information and numerical modeling could be found in a Lai et. al. (2015).

A systematic structural evaluation of the case study building indicated that the building failed to meet the performance objectives suggested by ASCE/SEI 41-13, *Seismic Evaluation and Retrofit of Existing Buildings* (ASCE 41, 2013). Similar outcomes were found using FEMA 351, *Recommended Seismic Evaluation and Upgrade Criteria for Existing Welded Steel Moment-Frame Buildings* (FEMA 2000), and FEMA P-58, *Seismic Performance Assessment of Buildings* (FEMA 2012a-c), showing that the building had a variety of seismic vulnerabilities, and suffered great damage and economic losses after basic safety earthquake hazard level (BSE) events. Consequently, feasible upgrade strategies are necessary to enhance the seismic performance of the building. The intent of the retrofit is to reduce the overall drifts of the structure to a level where brittle fracture of the beam-to-column connections would not seriously jeopardize the overall stability of the structure at a basic safety earthquake, level 2 (BSE-2E) hazard (with a probability of exceedance of 5% in 50 years). To achieve this, a “two-stage” retrofit plan was proposed. In “Stage-1”, the prevalent brittle column splices were fixed everywhere, and heavy concrete claddings were removed. The retrofit resulted in a change of elastic model periods, that were 4.33 sec. ( $X$ -direction translation), 4.18 sec. ( $Y$ -direction translation), and 3.59 sec. (rotation). Nevertheless, these strategies were demonstrated insufficient to achieve the target performance goal, and thus additional strategies are necessary. In “Stage-2”, three different kinds of supplemental energy dissipation devices were used in conjunction with strategies used in “Stage-1” for further improvement, including FVDs, VVDs and BRBs. This paper focuses on the “Stage-2” retrofits, and compares the cost-effectiveness of upgrading the case study tall building using selected devices.

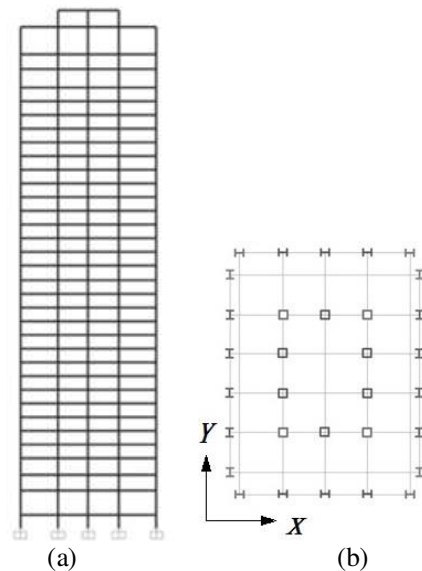


Figure 2. Illustration of the building model: (a) plane view of a typical frame in  $X$ -direction; (b) floor elevation

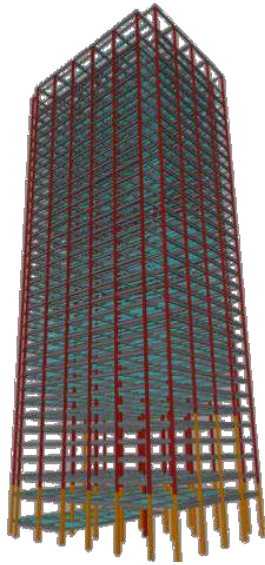


Figure 3. Illustration of the building model

### 03. Analysis Method

Nonlinear response history analysis (NRHA) was used to examine the seismic responses of the existing building using OpenSees. The retrofit feasibility study focused on BSE-2E hazard level. Three ground motions were selected at this hazard level for preliminary design and comparison, and the selection criteria was the closeness of their pseudo-acceleration spectra to the target spectra near the fundamental period of the original building, as shown in Fig. 4. “Stage-2” retrofit started with a numerical model with “Stage-1” retrofit, i.e., the column splices were fixed everywhere, and concrete cladding were removed. This baseline model was denoted as “as-built” hereafter.

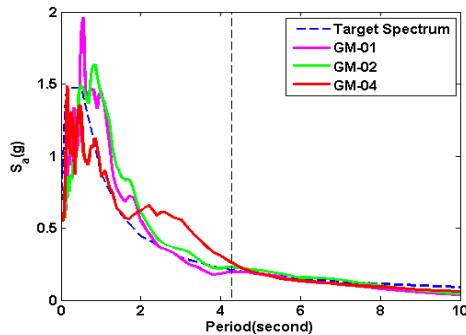


Figure 4. Target response spectrum and selected ground motions at BSE-2E

### 04. Retrofit with FVDs

The “Stage-2” retrofit plan started with design of FVDs. The locations for installing devices were selected considering the architectural restraints, constructability as well as damper

efficiency. Effective damping ratios were estimated based on the target roof displacement in each direction at BSE-2E events. The mechanical properties of dampers were selected using an equation related to the effective damping ratio, and story wise distributions of dampers. Several design considerations and viable alternatives to address these considerations were raised at the end of this section.

#### 4.1 Damper locations

To initialize the design within an existing building, the first consideration was selecting proper locations to install supplemental devices. Fig. 5 shows the plane view of a typical floor based on the architectural drawing, where the black boxes indicate column locations. The interior frames are usually adjacent to stairs and elevator locations, and putting dampers there would interfere with office space and egress. Therefore, the perimeter frames are considered as better options to add dampers. At first few trials, FVDs were installed along all stories with three different distribution patterns of the damping constant  $C$ : (I) uniform; (II) proportional to story shear; and (III) proportional to story stiffness. A preliminary analysis found that scheme (III), with damping constant  $C$  values proportional to story stiffness, was the most efficient among the three and thus selected for continued refinement. The initial design was refined by removing dampers, or adjusting damper sizes based on the control effectiveness of dampers at different regions. Consequently, a refined design scheme with concentrated dampers at lower two-thirds of the building was proposed; see Fig. 6. Damping exponent  $\alpha$  was set to be 0.35 to ensure adequate control effectiveness without excessive damper forces, based on a parametric study. In a single frame, dampers were distributed across multiple bays to minimize accumulation of forces transferred to the adjacent columns.

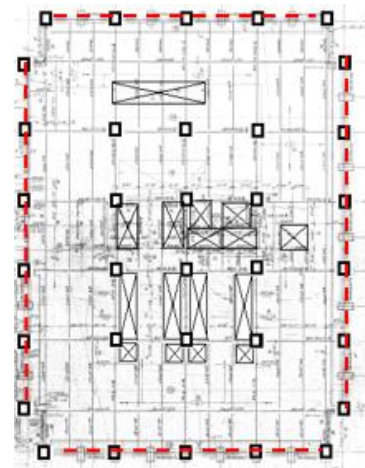


Figure 5. Openings at building floor

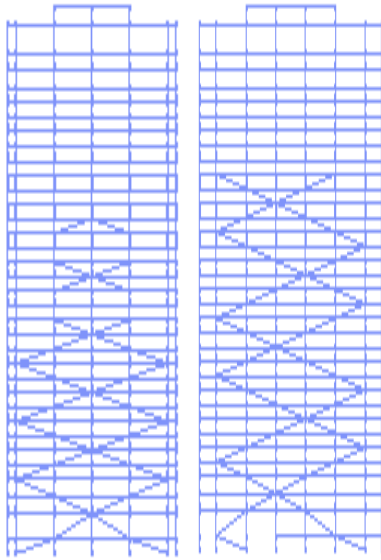


Figure 6. Story wise damper distributions

#### 4.2 Effective damping ratios

Estimating the overall effective damping (including the intrinsic damping and supplemental damping) needed to reduce the overall drifts is a prerequisite to estimate additional damping demand. A non-iterative approach was used based on researches of Rezaeian *et al.* (2012). In this approach, a Damping Scale Factor (DSF) was developed to adjust the 5% damped spectral ordinates to damping ratio ranging between 0.5% and 30%, which is defined as the ratio between the target overall displacement to the current displacement demand. The target roof displacement at each direction was selected based on the static pushover curves when the original building abruptly lost more than 70% force resistance capacity. Meanwhile the current displacement demands were estimated from the displacement spectrum at BSE-2E event. The DSF was then related to a regression relation derived based on the entire NGA-W2 earthquake record set (Rezaeian *et al.* 2012). Variations of magnitude, source-to-site distance and local site conditions have been considered in the regression relation. With a calculated DSF of each direction, the required damping ratios at a BSE-2E event were estimated, which were 8% for X-direction and 13% for Y-direction.

#### 4.3 Mathematical modeling

General fractional derivative Maxwell model was described by Makris and Constantinou (1990) to capture the behavior of FVDs, whereas a simplified mathematical model (Eq. (1)) could be used if the operating frequency is under the cut-off frequency of a FVD, that is, the stiffening effect of a FVD

during dynamic vibration is neglected (Constantinou and Symans 1992; Reinhorn and Constantinou 1995):

$$F_d = C v^\alpha \cdot \text{sign}(v) \quad (1)$$

where  $C$  is the damping constant,  $\alpha$  is the damping exponent, and  $\text{sign}(v)$  is the sign function of relative velocity of the piston end with respect to the damper housing. In earthquake engineering,  $\alpha$  is generally in the range of 0.3 to 1.0 (Lee and Taylor 2001). Eq. (1) could predict behaviors of a FVD well for low rate excitations, but the frequency-dependent contents need to be accounted as the operating frequency increases.

To model the FVD in OpenSees, a *viscous damper* material was used to represent the damper sub-assembly: a dashpot and a spring in series. The dashpot resembled the pure viscous behavior, as described by Eq. (1); the elastic spring element represented the driving braces. Researches (Fu and Kasai 1998; Takewaki and Yoshitomi 1998) have found that the brace flexibility would influence the damper behavior significantly and shall be fully accounted for. In this study, the total brace stiffness per story was equal to twice of the story stiffness, which was proven to be rigid enough to ensure adequate effect of FVDs.

#### 4.4 Design considerations

For a high-rise building, fairly large dampers are usually required to achieve the target performance goal, and this poses great challenges to existing buildings. Issues such as delivering heavy devices to multiple stories and clearing structural/non-structural components would increase construction difficulty and retrofit costs, and need careful considerations. Alternatives such as using two dampers per driver, more damped bays at selected stories, and utilizing toggle-brace mechanisms to magnify the effective force of a damping device (Taylor and Constantinou 1998) might be considered. On the other perspective, reduced performance objectives might be used.

Another critical design consideration is the vulnerable columns. After implementing “Stage-1” retrofits, the columns are anticipated to have adequate tension capacities, but they might still be overloaded in compression. Using FVDs could bring down the drift ratios and reduce the axial forces and bending moments in columns. Nevertheless, an excessive accumulation of damper forces on adjoining columns would cause problems if the structure enters into inelastic range, and the damper forces are large. Other factors such as the flexibility of connecting elements (e.g., driving braces, girders, connections and columns) would drive the dampers to act more in-phase with peak displacement and add up to the total forces in columns. Additional retrofit methods such as filling the columns with concrete, constructing mega columns at the corners might be investigated.

## 05. Retrofit with VWDs

The retrofit design scheme of using VWDs followed that of FVDs, and used consistent installation locations. The mathematical model and mechanical properties of VWDs are presented in this section. One of a unique design issue of VWDs is highlighted in the end.

### 5.1 Mathematical modeling

A Kelvin material model (Eq. 2) with linearized parameter could be used to simulate a viscoelastic damper with mild frequency-dependence (Lobo et. al. 1993):

$$F_d = Ku + Cv^\alpha \quad (2)$$

where  $C$  is the damping constant,  $\alpha$  is the damping exponent, and these two parameters of each VWD are kept the same as that of a FVD at the same location.  $u$  is the relative displacement of the two steel plates. Another parameter  $K$ , representing the storage stiffness of VWD tanks is introduced, which represents the capability of a VWD to provide additional stiffness. Recent tests on VWDs in the United States (Newell et. al. 2011) showed the stiffening of the structure due to wall dampers was about 5%, and thus the stiffness parameter  $K$  of 1000  $k/in$  was used for all VWD elements in this study for simplicity.

In the numerical model, a beam was modified if a VWD element was inserted into its middle span; see Fig. 7. First, an additional node was created in the central bay of a beam, and the beam was discretized into two elements. The alternation was made for both the upper and lower beams connected to a VWD. To model the VWD element, a two node link element was generated in OpenSees that connected the two middle nodes at upper and lower beams, and a *viscous damper* material model and an *elastic* material model were used in parallel to represent Eq. (2). The parameters of a *viscous damper* material were identical to the FVD element at each location, and the *elastic* material used a stiffness  $K$  equaling 1000  $k/in$ , as discussed before. The materials were applied in the direction of in-plane movement of the VWD. With introduced additional stiffness, the overall fundamental period of the case study building shifted from 4.33 sec. (have “Stage-1” retrofit only) to 4.10 sec.

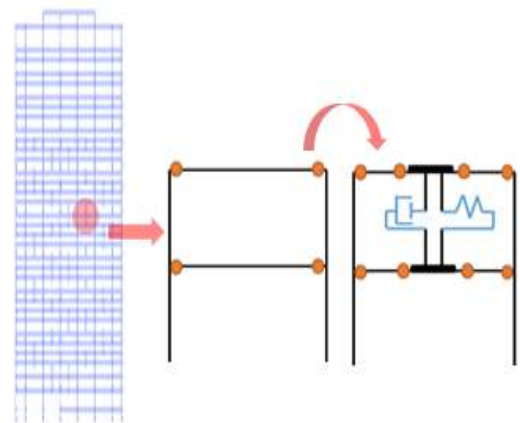


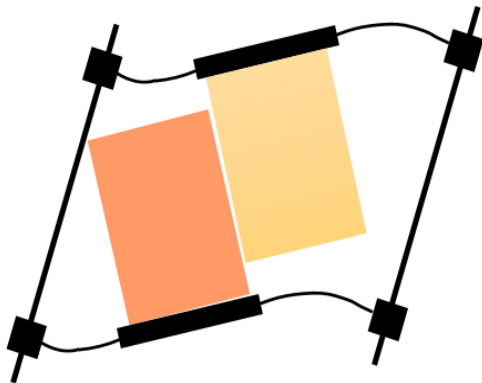
Figure 7. VWD modeling

### 5.2 Design considerations

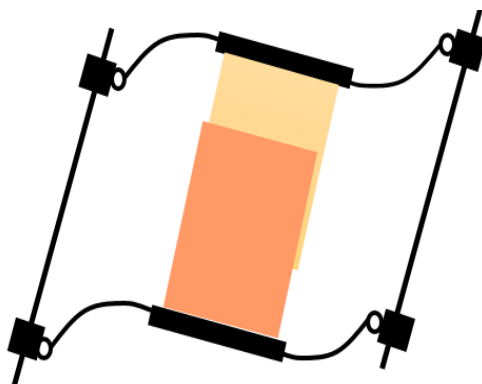
VWDs could provide more architectural flexibility than the brace-type dampers (e.g., FVDs, BRBs), and they could provide both additional damping and additional stiffness. However, several considerations call for special attention. As with the case to install FVDs, using VWDs would bring about similar design considerations such as the large damper sizes, vulnerable columns etc. Additionally, the effect of a VWD in the frame would be quite sensitive to the behaviors of beams connected with it. For an existing steel building having Pre-Northridge moment connection details, this problem is a bigger concern and thus presented below.

First of all, the effect of a VWD will be greatly influenced by the behaviors of beams connected with it. Fig. 8 shows the deformed shapes of a frame with two different cases. In case 1, if a beam is strong and could provide full restraint against bending, it would deform as an end fixed beam, and its deformed shape could produce large relative movement between two steel plates; see Fig. 8(a). Consequently, a large amount of energy dissipation would be produced. On the other hand, in case 2, the beams-to-column connections are released, and the beam would deform without rotational constraints. As such, the deformed shape of the upper and lower beams would limit the relative displacement between two steel plates, and result in insufficient energy dissipation of the VWD; see Fig. 8(b). Thereby, in order to ensure adequate energy dissipation provided by VWDs, the beams need to be strong and provide enough rotational constraints. However, the Pre-Northridge beam-to-column connections used in the case study building make it hard to meet this criterion, since a great many of these connections exhibited brittle failure (Lai et. al. 2015). Once the beam end connections fail, the beam would deform like case 2, significantly diminishing the energy dissipation capacity of the connected VWD element. It should also be highlighted that a sudden change of the deformed shapes upon the beam

failure might produce a spike of force and deformation on the VWD, and bring about the rupture of viscous material and the failure of the wall damper.



(a). Case 1: deformed shape with fixed-end connection



(b). Case 2: deformed shape with pin-end connection  
Figure 8. Deformed shape of a frame with different boundary conditions

Secondly, the storage stiffness of a VWD would affect the beam deformations. If the storage stiffness of a VWD under a dynamic loading is large, it would prevent the two steel plates moving freely (see Fig. 9), and resulted in reduced energy dissipation capacity of a VWD. Note that the storage stiffness of a VWD is not an exclusive contribution from the steel plates; the frequency-dependent part of the viscous material would also influence the storage stiffness (Fu and Kasai, 1998). More research is needed to understand the relation between the VWD storage stiffness, beam stiffness, and their effect on the behavior of the VWD.

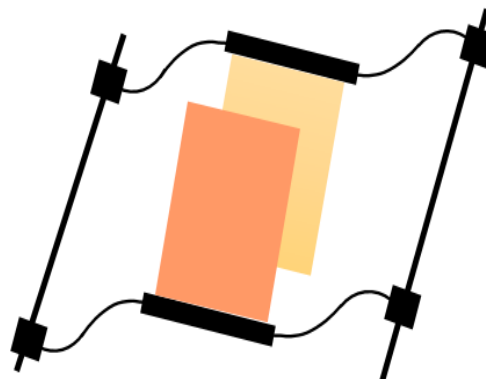


Figure 9. Deformed shape of a frame when the storage stiffness of a VWD is large

Thirdly, the seismic demands on the structural components would be increased with the additional stiffening effect, which in turn would cause an earlier fracture of beam-to-column connections. Both the bending moment demands and the shear demands would be increased. It should be noted that the increase of the shears also depends on the aspect ratio (defined as its width-to-depth ratio) of a VWD. The shear forces are amplified by the inverse of the aspect ratio. Thus if a small aspect ratio is used, beam would end up with large shear force, and suffer from shear yielding. Nevertheless, the numerical model did not include the shear yielding, and the results would be optimistic.

## 06. Retrofit with BRBs

BRBs are cheaper than FVDs or VWDs, and they are considered as ordinary braces in the U.S. design code, which make their design and analysis procedures less complicated than other supplemental energy dissipation devices. As with previous two retrofit methods, the distributions of BRBs in the existing building followed the pattern with FVDs and VWDs. In this section, the mathematic modeling of a BRB in OpenSees and the major design considerations would be discussed.

### 6.1 Mathematical modeling

BRB is a kind of displacement-dependent devices, and it dissipates energy through the yielding of the brace. The basic force-displacing relation of a BRB is expressed as:

$$F_d = Ku \quad (3)$$

where  $K$  is the effective stiffness of the brace, and  $u$  is the relative displacement between two ends of a brace. When a brace is in its elastic range,  $K$  represents the elastic stiffness. After it yields, a post-yield stiffness in the order of 0.001 of the elastic stiffness is used to represent its force resistant capacity. This strain hardening value of 0.001 is recommended in the OpenSees manual (Mazzoni *et al.* 2006),

which could control the transition from elastic to plastic branches and accounts for isotropic hardening.

To simulate the behavior of a BRB, a co-rotational truss element was used in OpenSees. The material model used a Giuffre-Menegotto-Pinto model (*Steel02*), and was assigned in the axial direction of the element. The effective stiffness  $K_0$  in the elastic range was estimated using the principle of equal energy dissipation. This was calibrated by assuming that the peak force  $F_0$  of a FVD and a BRB would be the same when they reached a same peak displacement  $U_0$ ; see Fig. 10. The proposed simple model was adequate to capture the primary characteristics of BRBs, e.g., the Bauchinger effect and strain hardening effect, and thus selected for this study. The stiffening effect of BRBs changed the fundamental period of the building from 4.33 sec. to 4.05 sec.

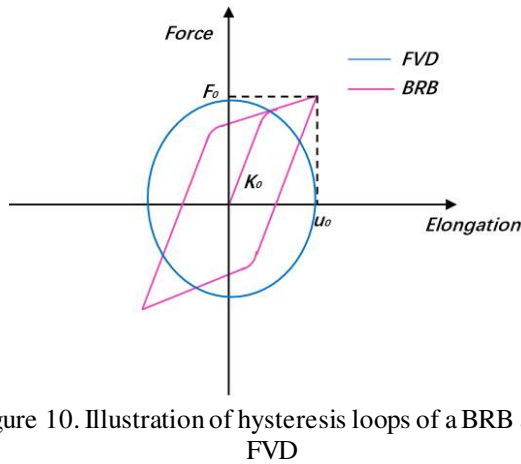


Figure 10. Illustration of hysteresis loops of a BRB and a FVD

## 6.2 Design considerations

When use BRBs, design considerations such as large peak forces of BRB devices, and overloaded columns exist, as with other retrofit methods. Nevertheless, their displacement-dependency would force BRBs to act more in-phase with peak displacement, and the peak force demands on existing beams and columns would be increased at a larger extend than other two methods.

## 07. Comparison of Control Effect

The results of global structural responses, damper/BRB behaviors, and column axial force status are presented for the “as-built” building with “Stage-1” retrofits only, and three retrofitted cases with different supplemental energy dissipation devices. The maximum results from three nonlinear response analyses are used, as stipulated by ASCE 41-13. Two horizontal directions are evaluated separately, while only the  $X$ -direction drift ratios and floor accelerations are shown for discussions, and the global responses in the  $Y$ -

direction follow a similar trend. It should be noted that during the simulation (entire ground motion duration plus 15-second free vibrations), most numerical simulations were successful; however, in the case with VWDs, several VWDs were broken under one ground motion excitation after the connected beams failed, and the structure had a peak drift ratio in excess of 10%. In this case, the numerical analysis was arbitrarily terminated since the building was most likely to collapse.

## 7.1 Global responses

The peak displacement distributions shown in Fig. 11 indicate that all cases incorporating different devices could help reduce the structural deformations by a large amount, ranging from 20% to 40%. With a same effective damping ratio, they help bring down the peak roof displacement to a similar value, and the value is close to the selected target roof displacement, i.e., 38 inches in the  $X$ -direction. This demonstrates that the DSF method discussed in Section 4.2 to estimate the effective damping ratio is adequate for preliminary design of FVDs.

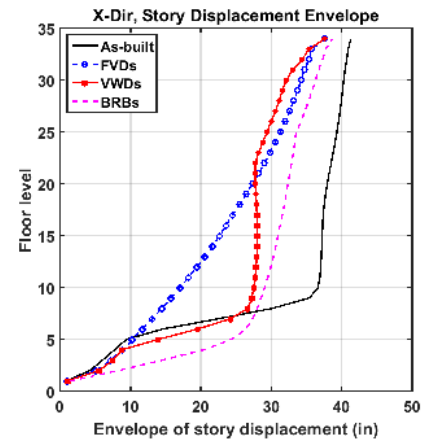


Figure 11. Distributions of peak displacement in  $X$ -dir.

Among three retrofit schemes, the strategy of using FVDs is considered as the most effective to eliminate the concentrated drift ratios at floor level 2-10, and contributes to a more uniform distribution of the peak deformations; see Fig. 12. On the other hand, the retrofitted schemes using VWDs or BRBs could not achieve satisfied control effect and still have a peak drift ratio in excess of 3% at floor 3 to floor 7. Such a large drift ratio indicates the latter two retrofitted methods are not able to meet the retrofit intent of maintaining structural stability at BSE-2E events.

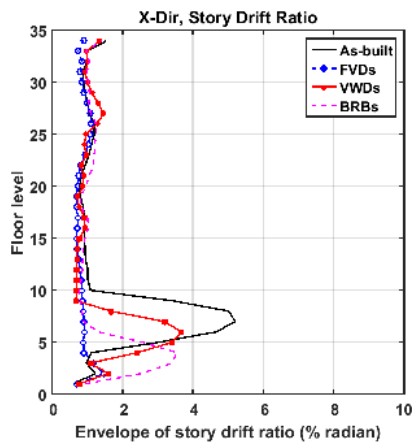


Figure 12. Distributions of peak drift ratio in X-dir.

The maximum peak floor accelerations are examined in Fig. 13. The “as-built” case has a peak floor acceleration of 0.85g at roof level. FVDs are able to reduce the peak floor accelerations by about 30% throughout the stories, and bring down the peak value at roof to 0.69g. The reductions benefit from the additional damping effect provided by FVDs, and the additional stiffening effect is not significant. On the other hand, the case installing VWDs provides limited control over the peak floor accelerations: the reduction is less than 10% over all the story levels, and is essential zero at roof level. The third case that uses BRBs is demonstrated to have the worst control effect, where the floor accelerations are increased at a majority of floor levels, and the peak roof acceleration is increased to 0.96g. This counter productivity of BRBs to control floor accelerations is mainly attributed to their displacement-dependent characteristics, which would increase the force demands and accelerations at each floor.

Similarly, the roof acceleration time history during free vibration phase in Fig. 14 shows that only FVDs could contribute to a more rapid decay of vibrations among three cases under investigation.

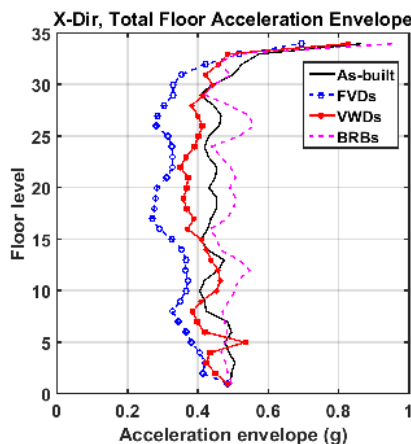


Figure 13. Distributions of peak floor accelerations

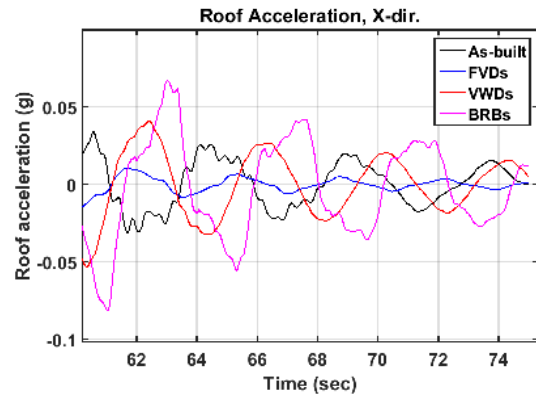


Figure 14. Time history of roof accelerations

## 7.2 Damper responses

In addition to the structural global responses, the peak force demands of each retrofit scheme are examined. The hysteresis loops of one device, located in Y-direction at the 3<sup>rd</sup> floor, subjected to one ground motion are plotted for different schemes; see Fig. 15. Under a same excitation, three devices have different behaviors. The FVD exhibits pure viscous properties, as shown by the elliptical shape of hysteresis loop. The VWD has steel tanks at the exteriors of the viscous material, thus having an increased load-resistant capacity. However, a BRB has a totally different energy dissipation mechanism compared to a FVD or a VWD. A BRB dissipates energy through the yielding of braces, and a typical hysteresis loop is represented by a bilinear curve. For the damper selected for investigation, the FVD dissipates most input energy despite that all three devices are designed to have a similar energy dissipation capacity. All different devices show a similar deformation level.

Meanwhile, the maximum damper force demands are shown for all schemes in Fig. 16. Fairly large force demands are observed for all cases, ranging from 1200 kips to 2300 kips. It should be noted that FVD scheme, the most effective to suppress the peak deformations and peak floor accelerations, turns to have the smallest peak force demands among the three.

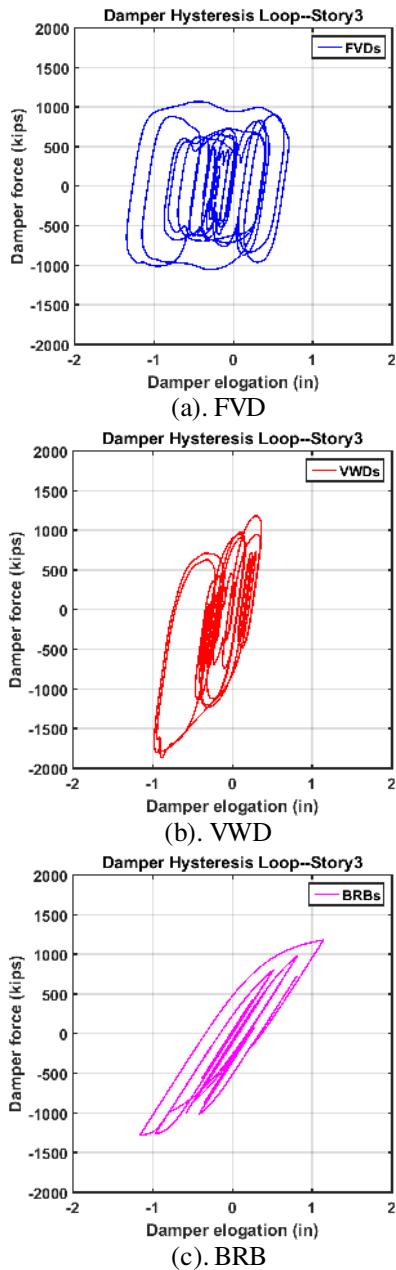


Figure 15. Hysteresis loops of one damper/BRB in story 3, Y-direction.

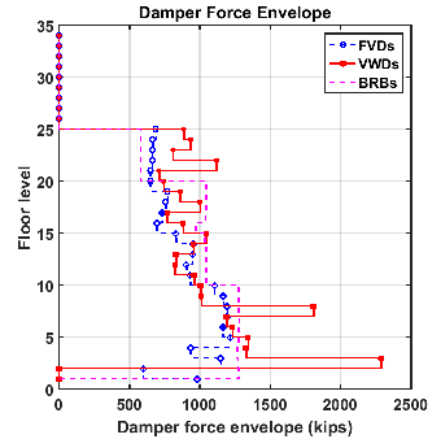


Figure 16. Distributions of peak force of each kind of device

### 7.3 Column axial force status

The evaluation of the case study building reveals that vulnerable columns have posed a great danger to the seismic integrity of the building. In the “Stage-1” retrofit, the brittle columns splices were fixed and thus the concerns of brittle column splice rupture/failure were eliminated. Nevertheless, on the compression side, the columns might be overloaded axially. Under a combined axial forces and bending moments, these columns are very sensitive to yielding, threatening the overall stability of the building. The introduction of supplemental energy dissipation devices could bring down the drift ratios demands, but the total force demands in the base columns would remain the same if the seismic input does not change. In the case having VWDs or BRBs, the seismic demands are increased due to their additional stiffening effect. As such, the axial force demands on base columns would increase, exacerbating the column conditions.

To evaluate the influence of supplemental devices on the columns, the envelopes of axial force demand-to-capacity ( $D/C$ ) ratio are examined for one group of exterior corner columns. The selected columns fall into Group 1, identified in Fig. 17, which have built-up W-sections. These corner columns are usually most heavily loaded under selected seismic excitations. The “Stage-1” methods have strengthened the column splices, the columns tension capacities are thus estimated based on Equation 9-8 of ASCE 41-13, i.e.,  $P_t = A_g \times F_y$ , where  $A_g$  is the gross section of columns, and  $F_y$  is the expected yield strength of the material. On the compression side, the buckling of columns is considered and the lower bound compression capacities are calculated:  $P_c = A_g \times F_{cr}$ , where  $F_{cr}$  is the material strength considering global buckling.

The positive sign is for tension while the negative sign signifies compression in Fig. 18. The green line is the

compression demands due to gravity force, which consumes about 30% of the column compression capacities. For the “as-built” case, the peak  $D/C$  exceeds 1.0 at floor 6-7, and there are more than half of stories having peak  $D/C$  ratios larger than 0.5. At these levels, ASCE 41 indicates that the members should be treated to be force controlled and remain elastic. The high  $D/C$  ratios at most floor indicate a significant reduction of column bending capacities, which would likely contribute to the weak column, strong beam behavior observed in the results. On the other hand, tension rupture/failure is typically not a concern with all the brittle splices fixed.

For the case with FVDs, the peak  $D/C$  ratios are reduced slightly at several floors on tension, though there are no significant reductions of compression forces. Nevertheless, neither VWDs nor BRBs are able to alleviate the high column axial forces. The axial  $D/C$  ratios at most floors are increased instead, and widespread column failures are more likely in both cases. Other strategies to upgrade the column capacities, such as filling concrete in the built-up section columns, or adding corner columns could be explored.

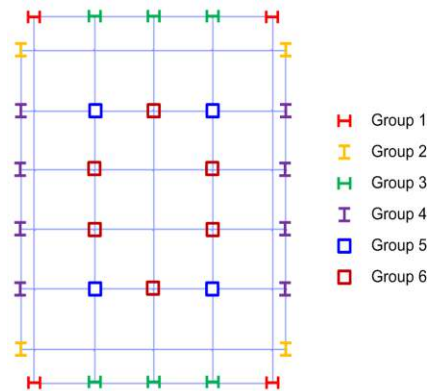


Figure 17. Column group designations

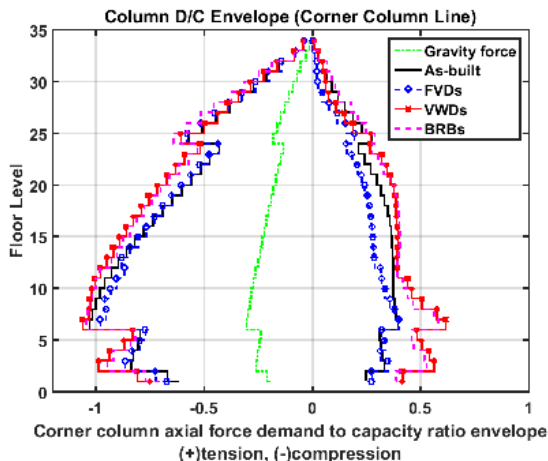


Figure 18. Distributions of column axial  $D/C$  ratios

## 08. Damage and Loss Analysis

The damage and loss analysis was conducted using the software developed by FEMA: Performance Assessment Calculation Tool (PACT). The PACT performs the probabilistic loss calculations in the framework of Performance Based Earthquake Engineering (PBEE). The repair cost and repair time of each realization were estimated from fragility curves of structural and non-structural components, and consequence functions of damaged components. Four engineering demand parameters were used to predict the damage states of different components, including the peak story drift ratios, peak floor accelerations, peak floor velocities and maximum residual drift ratios. Among these, the first three parameters were results from nonlinear response history analyses, while the residual drift ratios were estimated based on an empirical relation suggested by FEMA P-58 (FEMA 2012a).

The probability of the building having irreparable residual drifts and the probability of unsafe tagging at BSE-2E event for the “as-built” building and three fully retrofitted buildings are summarized in Table 1. The “as-built” one is expected to have very large residual drift ratios at BSE-2E events, making repair work unsafe and unrealistic. This could be seen from the high chances of irreparability and high probability of unsafe tagging of the “as-built” case. It is most likely that a complete tearing down and reconstruction are necessary. As a comparison, the building inserting FVDs successfully brings down the residual drifts, and it has only 0.6% chance of being irreparable. A 26.9% of unsafe tagging is estimated, which is mainly resulted from failure of Pre-Northridge beam-to-column connections and prefabricated steel stairs. Consistent with what have been observed from structural analysis results, the other two retrofit methods by using either VWDs or BRBs still exhibit large residual drifts, and are less effective to reduce the chance of tearing down the building, nor the chance of unsafe tagging at BSE-2E.

To better assess each retrofit scheme, the cumulative distribution curves of repair loss ratio are presented and compared; see Fig. 19. The repair loss ratio is defined as the repair cost divided by the building’s replacement cost according to FEMA P-58 (2012a). The replacement cost of this building is the reconstruction fees, and is estimated to be \$475 million based on recent market values of similar buildings in San Francisco area (Kidder Mathews 2015). From the cumulative distribution curves, the median values and 90 percentile values are extracted and listed in Fig. 20. Both the “as-built” case and the VWDs case have a median loss ratio equal to 1.0, i.e., the building needs full replacement after a BSE-2E event for these cases. The retrofit scheme with BRBs brings down the median loss ratio to about 0.084, but still hits 1.0 when a larger confidence

level (90 percentile) is assessed. On the contrary, the retrofit scheme using FVDs avoids large economic losses, and reduces the median repair loss ratios to 0.047, and 90 percentile value to 0.071.

The overall cost-benefit of each retrofit scheme needs to include the costs associated with purchasing and implementing supplemental energy dissipation devices in the building. The initial costs of purchasing various supplemental energy dissipation devices from manufactures are estimated in Table 2. These costs are a rough estimation based on available online data and consultation from experienced engineers, since real data is usually confidential and not easy to approach. BRB is the cheapest, and VWD is the most expensive device. Additional installation fees such as construction cost to strengthen existing structural elements/connections, transportation cost of heavy devices to higher floors, and cleaning fees to save space for supplemental devices need to be fully accounted. Nevertheless, it would be rather difficult to estimate this budget considering large uncertainty of above mentioned items. As such, a simple calibration is proposed by using an amplification factor, which is multiplied by the initial device costs to represent the total investment of each retrofit scheme. An amplification factor of 10 is used considering the size of the case study building, its importance and quantity of devices. The cost efficiency of different retrofit methods at BSE-2E event are compared in Table 3. The FVDs retrofit method is considered to be the most cost-efficient to upgrade the case study building since it has more than 50% chance to save \$452 *M* repair cost, and more than 90% chance to save \$441 *M* after a BSE-2E event. Meanwhile, the initial investment of \$84 *M* is relatively small compared with its potential savings. The case using BRBs ranks the second since it has the minimum initial investment of \$17 *M*, and has more than 50% chance of saving \$435 *M* repair cost at a BSE-2E event. Nevertheless, no benefits are expected if a higher confidence level of 90% is to be achieved. Lastly, there is more than 50% chance that VWDs would not save repair cost, and its initial investment is the largest. Thus VWD is the least cost-effective method.

Table 1. Loss estimates

| Scenario | Probability of irreparability | Probability of unsafe tagging |
|----------|-------------------------------|-------------------------------|
| As-built | 94.3%                         | 98.3%                         |
| FVDs     | 0.6%                          | 26.9%                         |
| VWDs     | 66.0%                         | 70.6%                         |
| BRBs     | 45.5%                         | 60.6%                         |

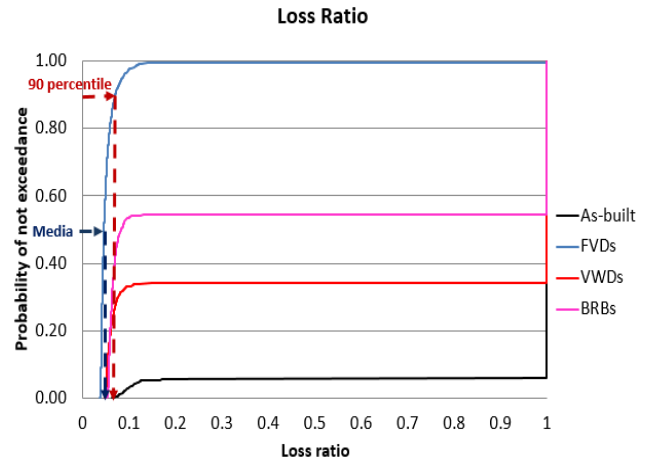


Figure 19. Cumulative distribution curve of loss ratio

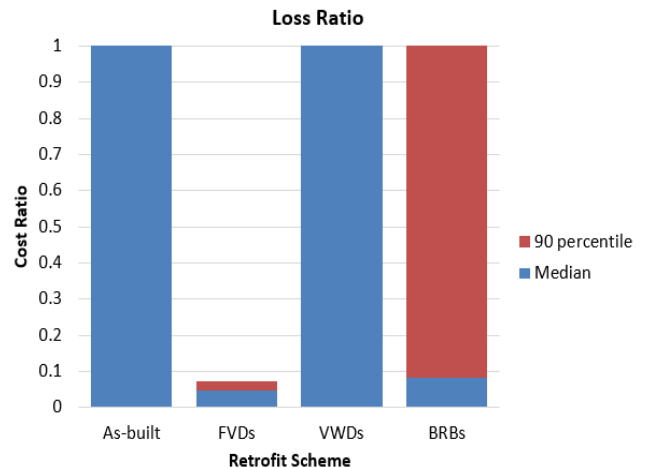


Figure 20. Median and 90 percentile loss ratio

Table 2. Estimated initial costs of various devices

| Scheme | Initial Cost (\$M) |
|--------|--------------------|
| FVDs   | 6.4                |
| VWDs   | 8.4                |
| BRBs   | 1.7                |

Table 3. Cost benefit comparison

| Scheme   | Investment (\$M) | Benefit from savings (\$M) |                |
|----------|------------------|----------------------------|----------------|
|          |                  | Median                     | 90 percentiles |
| As-built | 0                | 0                          | 0              |
| FVDs     | 64               | 452                        | 441            |
| VWDs     | 84               | 0                          | 0              |
| BRBs     | 17               | 435                        | 0              |

## 09. Conclusions

A representative Pre-Northridge high-rise steel moment resisting frame was selected for seismic performance assessment. The evaluations were based on ASCE 41-13 procedures FEMA 351 and FEMA P-58, and identified several major structural vulnerabilities of the case study building. As such, possible retrofit methods as well as their cost-effectiveness were explored. A “two-stage” retrofit plan was proposed for the case study building. In “Stage-1”, the brittle column splices were fixed everywhere, and the exterior heavy claddings were removed. However, analysis results indicated that “Stage-1” method alone was not enough to meet the retrofit goal of maintaining structural stability at a BSE-2E event. Therefore, in “Stage-2”, several supplemental energy dissipation devices were used in combination with “Stage-1” methods to further enhance the building’s seismic performance. The control effect, in particularly the cost-effectiveness of each retrofit method is investigated and compared in this paper.

Three devices are investigated in this paper: FVDs, VWDs and BRBs. The design started by designing FVDs. Four perimeter frames were selected to install these devices so that the interaction of occupants and interior components could be minimized. The total effective damping ratios were estimated to achieve the target roof displacements at each horizontal direction. A refined damper design was proposed where dampers were installed only in locations with better control effectiveness. These locations were the same for all retrofitted schemes using different energy dissipation devices. In addition, the mechanical properties of three devices were selected based on the assumption of equal energy dissipation.

The structural global responses, devices behaviors and column axial force status are presented. The results presented are the maximum values from three nonlinear response history analyses at BSE-2E. The global responses show that the FVDs are the most effective to bring down the drift concentrations at floor level 2 to 10, and result in a more uniform distribution of the peak deformations. The peak drift ratio after installation of FVDs is less than 1.5%, which could essentially eliminate the beam-to-column connections failure at BSE-2E events. FVDs are also shown to be the most efficient to suppress the peak floor accelerations and contribute to a more rapid decay of the structural vibrations. For other two retrofitted cases using VWDs or BRBs, unique problems are found and neither of them is able to provide effective structural control to the building under seismic excitations, and thus unable to meet the retrofit goal. Specifically, the introduction of a VWD in the middle of a beam having Pre-Northridge connection details would cause an earlier fracture of beams, and the control effect of VWDs would be significantly diminished once a large number of

beams fail. The displacement-dependent BRBs are acting in-phase with structural displacements, and increase the force demands to existing members. Besides, both VWDs and BRBs provided additional stiffness, reducing the building’s fundamental period and increasing the seismic force demands.

In addition, the behaviors of dampers or BRBs are checked. The results indicate that fairly large devices are required in all schemes, while the sizes of FVDs needed are anticipated to be the smallest despite of their best control effects among the three schemes. To relate the structural performance to the economic losses, a damage and loss analysis is conducted following procedures outlined in FEMA P-58. The results are consistent with the structural analyses, indicating that FVDs are the most effective to reduce the probability of having irreparable residual drifts, probability of unsafe tagging, and led to much reduced economic losses after a BSE-2E event from the “as-built” case. BRBs help improve the structural behavior a little, but are insufficient to provide a high confidence level of 90% to reduce repair cost. On the other hand, VWDs provide little, if any, contributions to reducing the economic consequences after a BSE-2E event due to a great number of beam failure and diminished damper effect.

Several design considerations exist for each scheme. One common issue among three cases is the widespread vulnerable columns in the building. Even after the brittle splices were fixed, the columns are overloaded in compression and sensitive to yielding under combined axial force and bending. This poses great threat to the seismic integrity of the building, and additional methods to upgrade columns should be explored.

In summary, among three energy dissipation devices investigated, FVDs have the least interaction with structural members, and are able to introduce additional damping without significantly increasing the structural demands on the vulnerable columns and beams. Therefore, they are viewed as the most promising solution to improve the structural behavior and reduce the economic losses of a Pre-Northridge high-rise steel moment resisting frame.

## Acknowledgement

This paper is supported by Pacific Earthquake Engineering Research center (PEER) as part of its Tall Building Initiative and Next-Generation Attenuation Relationship programs. Special thanks to Dr. Jiun-Wei Lai and Dr. Matthew Schoettler who dedicated to set up the OpenSees model, as well as the assistance from Dr. Frank McKenna, Dr. Andreas Schellenberg and Prof. Dimitrois Lignos to refine the numerical model. The authors would also like to express great gratitude to Prof. Kazuhiko Kasai of Tokyo Institute of

Technology, Dr. Kit Miyamoto and Dr. Amir Gilani of Miyamoto International, Dr. Amarnath Kasalanati of Dynamic Isolation Systems, Jim Malley of Degenkolb Engineers and Rob Smith of Arup for sharing their valuable expertise and advice.

## Reference

- AISC (2010). *Specification for Structural Steel Buildings*, American Institute of Steel Construction, Chicago, IL.
- ASCE (2013) *Seismic Evaluation and Retrofit of Existing Buildings*, American Society of Civil Engineers, ASCE/SEI 41-13, Reston, VA.
- Constantinou M. C., Symans M. D. (1992). Experimental and analytical investigation of seismic response of structures with supplemental fluid viscous dampers, *NCEER-92-0032*, National Center for Earthquake Engineering Research, Buffalo, NY.
- FEMA (2000). *Recommended Seismic Evaluation and Upgrade Criteria for Existing Welded Steel Moment-Frame Buildings*, Federal Emergency Management Agency, FEMA 351 report, Washington, D.C.
- FEMA. (2012a): Seismic Performance Assessment of Buildings, Volume 1 – Methodology. Federal Emergency Management Agency, *FEMA P-58-1 report*, Washington, D.C.
- FEMA (2012b). Seismic Performance Assessment of Buildings, Volume 2 – Implementation Guide, Federal Emergency Management Agency, *FEMA P-58-2 report*, Washington, D.C.
- FEMA (2012c). Seismic Performance Assessment of Buildings, Volume 3 – Supporting Electronic Materials and Background Documentation, Federal Emergency Management Agency, *FEMA P-58-3 report*, Washington, D.C.
- Fu Y., Kasai K. (1998). Comparative study of frames using viscoelastic and viscous dampers, *Structural Engineering*, 124:513-552.
- Kidder Mathews (2015). San Francisco office real estate market review 3<sup>rd</sup> quarter 2015, retrieved March 2016, from <http://www.kiddermathews.com/downloads/research/office-market-research-san-francisco-2015-3q.pdf>.
- Lai, J.-W., Wang, S. Schoettler, M. and Mahin S. (2015). Seismic performance assessment of a tall building having Pre-Northridge moment-resisting connections, *PEER Report No. 2015/14*, Pacific Earthquake Engineering Research Center, University of California, Berkeley, CA.
- Lee D. and Taylor D. P. (2001). Viscous damper development and future trends, *J. Struct. Des. Tall Buil.*, 10, 311-320.
- Lobo, R.F., Bracci, J.M., Shen, K.L. et al., Reinhorn, A.M., and Soong, T.T. (1993). Inelastic response of reinforced concrete structures with viscoelastic braces, *Report No. NCEER-93-0006*, National Center for Earthquake Engineering Research, Buffalo, State University of New York at Buffalo, Buffalo, N.Y.
- Makris N., and Constantinou M.C. (1990). Viscous dampers: testing, modeling and application in vibration and seismic isolation, *Report No. NCEER-90-0028*, National Center for Earthquake Engineering Research, State University of New York at Buffalo, Buffalo, NY.
- Mazzoni, S., McKenna, F., Scott, M.H., and Fenves, G.L. (2009). Open system for earthquake engineering simulation: User command-language manual, Pacific Earthquake Engineering Research Center, University of California, Berkeley, OpenSees version 2.0 users' manual, retrieved from <http://opensees.berkeley.edu/OpenSees/manuals/usermanual/>, August, 2016.
- McKenna, F., Scott, M., and Fenves, G. (2010). Nonlinear finite-element analysis software architecture using object composition, *J. Comput. Civil Eng.*, 24(1): 95-107.
- Newell J., Love J., Sinclair M., Chen Y-N., and Kasalanati A. (2011). Seismic design of a 15-story hospital using viscous wall dampers, *Proceedings of Structural Congress*, Las Vegas, Nevada, U.S.
- Reinhorn A. M., Li C., Constantinou M. C. (1995): Experimental and analytical investigation of seismic retrofit of structures with supplemental damping, part I: fluid viscous damping devices. *NCEER-95-0001*, National Center for Earthquake Engineering Research, State University of New York at Buffalo, Buffalo, NY.
- Rezaeian S., Bozorgnia Y., Idriss I.M., Campbell K.W., Abrahamson N.A., Silva W.J. (2012). Spectral damping scale factors for shallow crustal earthquakes in active tectonic regions, *PEER Report No. 2012/01*, Pacific Earthquake Engineering Research Center, University of California, Berkeley, CA.
- Soong T. T., Spencer B. F. (2002). Supplemental energy dissipation: state-of-the-art and state-of-the-practice. *Eng. Struct.*, 24, 243-259.

Takewaki I. and Yoshitomi S. (1998). Effects of support stiffness on optimal damper placement for a planar building frame, *J. Struct. Des. Tall Buil.*, 7: 323-336.

Taylor, D.P., Constantinou, M.C. (1998). Development and testing of an improved fluid damper configuration for structures having high rigidity, *Proceedings of the 69th Shock and Vibration Symposium*, St. Paul, MN.